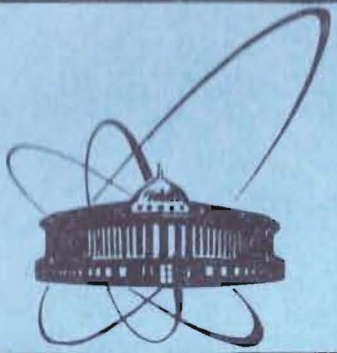

объединенный
институт
ядерных
исследований
дубна

E1-85-415

A.M.Baldin, L.A.Didenko, V.G.Grishin,
A.A.Kuznetsov, Z.V.Metreveli*

UNIVERSALITY OF HADRON JETS IN SOFT AND HARD PARTICLE INTERACTIONS AT HIGH ENERGIES

Submitted to the International Europhysics Conference on High Energy Physics (Bari, Italy, 1985), to the III All-Union Problematic Seminar on Interactions of High Energy Particles and Nuclei with Nuclei (Tashkent, USSR, 1985) and to the "Zeitschrift für Physik A"

* IHEP, Tbilisi State University

1985

1. INTRODUCTION

Recently the hadron jets produced in hard and soft processes in hadron-hadron interactions have extensively been studied.

The results are compared with analogous data for e^+e^- annihilation and deep inelastic scattering of leptons on nucleons [1-3]. This is due to the fact that the hadronization of quarks and gluons in e^+e^- annihilation as well as in muon and neutrino interactions with nucleons are studied well enough, and such comparisons allow one to establish common features and differences in the hadrons formation mechanism for various types of interactions.

The study of hadron jet production in cumulative hadron-nucleus interactions is of great interest [4-6]. Experiments on the study of the limiting fragmentation of nuclei, show that the nuclei are characterized by their own quark-parton structure function [4-6], which points to the existence of multi-quark configuration in nuclei.

The quark hadronization from the multiquark configurations in nuclei is naturally expected to lead also to hadron jet production.

The separation of such jets and the comparison of their properties with those of the hadron jets for different types of interactions, can give information on the particular features of the quark hadronization mechanism in nuclei.

The results of comparison of the hadron jet properties in soft π^-p- and cumulative π^-C-interactions at 40 GeV/c with the data on e^+e^- annihilation and $\nu(\bar{\nu})$p-collisions are given in this paper. The experimental data have been obtained using a 2m propane bubble chamber exposed to a beam of 40 GeV/c π^- mesons at the Serpukhov accelerator. The work has been done on statistics of 14000 π^-p and 8791 π^-C events*. The experimental technique is described in detail in papers [7-9].

* Interactions
the nucleus are

2. ANALYSIS OF THE HADRON JET BEHAVIOUR IN π^-p INTERACTIONS AT P = 40 GeV/c

2.1. Comparison of the Hadron Jet Characteristics in π^-p Interactions with the e^+e^- Annihilation Data

The analysis of the jet behaviour of secondary particles is performed in the π^-p c.m.s. by means of known variables, "sphericity" (S) and "thrust" (T):

$$S = \frac{3}{2} \min \frac{\sum_i P_{\perp i}^2}{\sum_i \vec{P}_i^{\,2}}, \qquad (1)$$

$$T = \max \frac{\sum_i |P_{||_i}|}{\sum_i |\vec{P}_i|}, \qquad (2)$$

where $P_\perp$ and $P_{||}$ are the transverse and longitudinal momenta of secondary particles relative to the jet axis [10,11]. Diffraction events were excluded from the analysis*.

Figure 1 presents the energy dependence of the average values of the variable $\langle S \rangle$ in the c.m.s. for e^+e^- interactions with $n_\pm \geq 4$ [11-15]. The same figure shows an average value of $\langle S \rangle$ for π p interactions ($E_{c.m.s.} = \sqrt{s} = 8.7$ GeV) with and without the account of the diffraction events.

The variable $\langle S \rangle$ for π^-p interactions is in good agreement with the existing energy dependence of $\langle S \rangle$ for e^+e^- interactions [14].

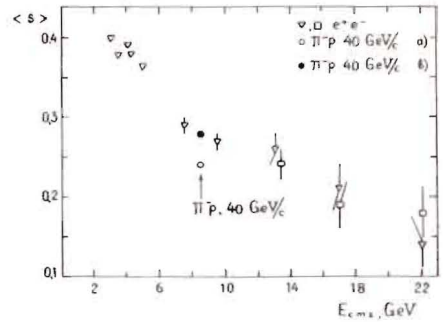

Fig.1. Dependence of average values of sphericity $\langle S \rangle$ on energy in the e^+e^- c.m.s.; Λ - PLUTO collaboration, □ - TASSO collaboration; ●, ○ - average values of sphericity in π^-p - interactions at 40 GeV/c; a) for all events; b) after excluding diffraction processes.

A difference for π^-p and e^+e^- interactions is observed in jet axis orientation relative to the primary direction of colliding particles. The distributions of events over $|\cos\theta|$, where θ is

* The event was considered to be a diffraction one if, at least, one charged secondary particle has $|x_F| > 0.8$ ($x_F = 2P_{||}/\sqrt{s}$).

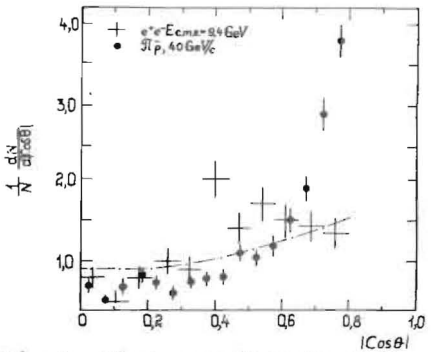

Fig.2. The $|\cos\theta|$ distributions of events where θ is the angle between the jet axis (the axis was defined relative to the variable "thrust") and the direction of colliding particles for e^+e^- annihilation at $E_{c.m.s.} = 9.4$ GeV and for π^-p interactions without diffraction component. The dashed line shows the $d\sigma/d|\cos\theta| = 1+\cos^2\theta$ dependence.

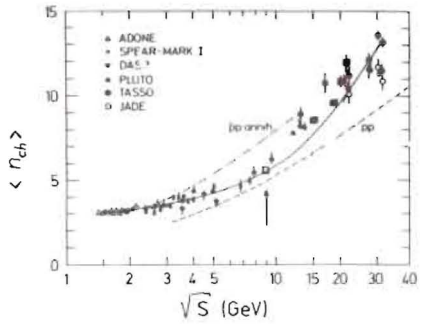

Fig.3. Dependence of the average multiplicity of charged particles, $<n_{ch}>$, on energy in the c.m.s. ($\sqrt{S}$) in e^+e^-, π^-p (□) and cumulative π^-C interactions (■). The solid curve is the prediction of the QCD for e^+e^- annihilation

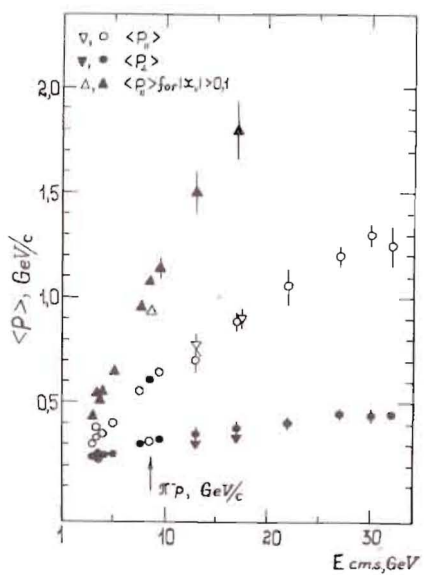

Fig.4. Dependence of average values of the transverse and longitudinal momentum of secondary particles relative to the jet axis on energy in the e^+e^- c.m.s. ●, ○ – PLUTO collaboration, ▼, ▽ – TASSO collaboration; ▲ – average values of the longitudinal momentum of secondary particles for $|x_F| > 0.1$ $<P_\perp>$ and $<P_\parallel>$ values, corresponding to π^-p interactions at 40 GeV/c are shown by an arrow; Δ and ▲ correspond to average values of $<P_\parallel>$ for $|x_F| > 0.1$ obtained without and with the diffraction processes.

the angle between the jet axis (the axis was defined by the variable "thrust") and the primary direction for both types of interactions, are presented in fig.2. The jet axis in π^-p interactions is oriented mainly at small angles to the direction of colliding particles ($<\theta> = 19.1 \pm 0.1$). This is just defined by the character of the soft collisions.

Figure 3 illustrates the dependence of the average multiplicity of charged secondary particles ($<n_{ch}>$) on the total energy in the c.m.s. for e^+e^- annihilation [12]. The arrow shows the value of $<n_{ch}>$ for π^-p interactions. The values of $<n_{ch}>$ are similar for both types of collisions.

The comparison of the average momentum characteristics of secondary particles relative to the jet axis is also of great interest. The average pion momenta $<P_\perp>$ and $<P_\parallel>$ in e^+e^- interactions relative to the jet axis are presented in figure 4 [9,12] for variable energies in the c.m.s. The same figure gives similar data for π^-p collisions at 40 GeV/c after excluding diffraction processes. They are in agreement with the data for e^+e^- annihilation at equal energies in the c.m.s.

Thus it can be concluded that the formation of two hadron jets, collimated in the direction of motion of colliding particles in their c.m.s., is observed in π^-p interactions at 40 GeV/c. The considered characteristics of these jets are similar to analogous data for e^+e^- annihilation.

2.2. Inclusive Characteristics of Particles in Jets

It is of interest to compare the one-particle inclusive distributions of charged secondary particles relative to the jet axis with analogous data for e^+e^- annihilation.

Figures 5 and 6 present the distributions of π^+ mesons for the forward hemisphere and of π^- mesons for the backward hemisphere over the variable $x_F = 2P_\parallel/\sqrt{s}$ calculated relative to the jet axis. They are compared with analogous distributions for e^+e^- annihilation at an energy of 7.4 GeV in the c.m.s. [16-17]. As is seen from the figures, in the forward hemisphere the distributions for both types of interactions practically coincide whereas in the backward hemisphere they are in agreement only in the region $x_F \geq -0.2$. Such a difference is likely to be due to the fact that the diquark fragmentation ($x_F < 0$) in π^-p interactions differs from the quark fragmentation ($x_F > 0$).

To analyse differences of quark and diquark fragmentations into pions, it is of interest to compare the data on π^-p interactions with data on deep inelastic $\nu(\bar{\nu})p$ scattering.

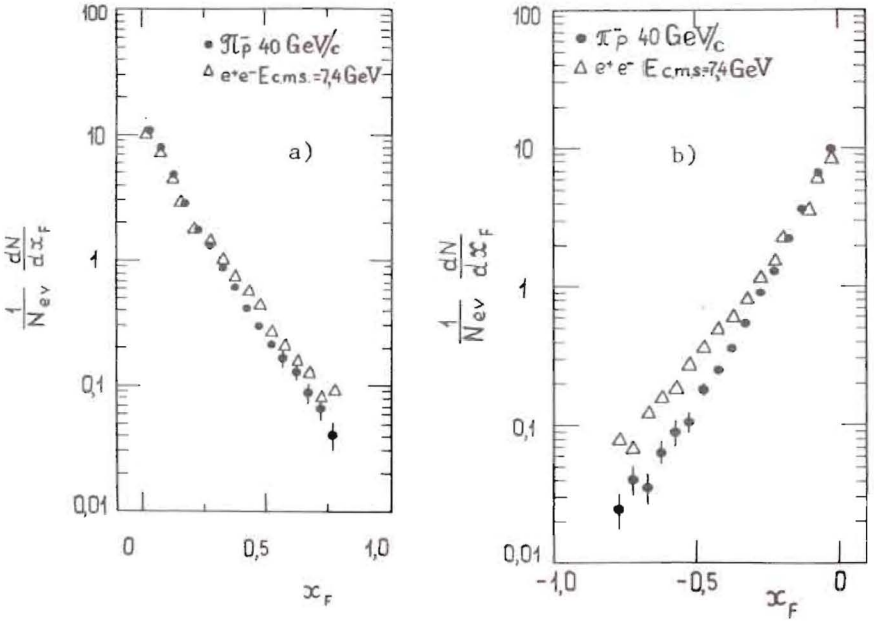

Fig. 5. The x_F distributions of secondary particles relative to the jet axis; Δ – for e^+e^- annihilation ($\sqrt{S}$ = 7.4 GeV); • – for π^-p interactions ($\sqrt{S}$ = 8.7 GeV); a) for π^+ mesons in the forward hemisphere; b) for π^- mesons in the backward hemisphere.

2.3. Quark and Diquark Fragmentation

Figure 6 presents the simplest diagrams of π^-p, $\nu(\bar{\nu})$p interactions and e^+e^- annihilation [18,19].

In a first approximation, one can assume that for π^-p interactions particles are mainly produced due to the fragmentation of noninteracting $\bar{u}$ or d quarks at $x_F \geq 0.1$ and due to the fragmentation of (uu) or (ud) diquarks at $x_F \leq -0.1$. For $|x_F| \geq 0.1$ the contribution from quark-quark interactions in hadron-hadron collisions is assumed to be small [18].

Comparing the quark and diquark fragmentations for different processes, we can apply the fragmentation $D(x_F)$ and invariant $F(x_F)$ functions:

$$D(x_F) = \frac{1}{N_{ev}} \frac{dN}{dx_F}, \qquad (3)$$

$$F(x_F) = \frac{1}{\sigma_{ev}} \int E \frac{d\sigma}{dp^3} dP_\perp^2 = \frac{1}{N_{ev}} \frac{E^*}{\pi P^*_{max}} \frac{dN}{dx_F} \xrightarrow{x_F \to 1} \frac{1}{r} |x_F| D(x_F) \qquad (4)$$

where $x_F = P^*_{||}/P^*_{max}$, N_{ev} is the number of events, N is the number of particles in these events, P^*, E^* are the momentum and energy of the considered hadron in the c.m.s.

Comparing the diagrams of the π^-p and $\nu(\bar{\nu})$p interactions (fig.5a,b) and assuming that the light quarks $\bar{u}$ and d interact with the same probability, the following relations can be written for the fragmentation functions (formula (3))*

$$D^{\pi^\pm}_{\pi^-p}(x_F) = \frac{1}{2} D^{\pi^\mp}_{\nu p}(x_F) + \frac{1}{2} D^{\pi^\pm}_{\bar{\nu}p}(x_F) \quad \text{for} \quad x_F \geq 0.1, \qquad (5)$$

$$D^{\pi^\pm}_{\pi^-p}(x_F) = \frac{1}{3} D^{\pi^\pm}_{\nu p}(x_F) + \frac{2}{3} D^{\pi^\pm}_{\bar{\nu}p}(x_F) \quad \text{for} \quad x_F \leq -0.1. \qquad (6)$$

The same relations should also be valid for the invariant functions $F^{\pi^\pm}(x_F)$ (formula (4)).

To compare the K^N meson and Λ hyperon characteristics in π^-p and e^+e^- interactions, the inclusive cross sections $\frac{1}{\beta}\frac{d\sigma}{dx_E}$ can be applied, where the Lorentz-factor

$\beta = P^*/E^*$ and $x_E = 2E^*/\sqrt{s}$ [18,20] **.

a) Quark fragmentation into $\pi^\pm$ mesons

Figure 7 presents $D^{\pi^\pm}(x_F)$ at $x_F > 0$ for π^-p and $\nu(\bar{\nu})$p interactions (formula (6)) normalized to the region $x_F \geq 0.1$. As is seen, the distributions obtained agree well with one another excluding the region $x_F \leq 0.15$ in which the contribution from interacting quarks in π^-p interactions is substantial (fig.6a).

Approximating the fragmentation functions by the expression:

$$D^{\pi^\pm}(x_F) = A \exp(-B|x_F|) \qquad (7)$$

we obtain that the values of the parameters A and B are approximately equal for both processes (table 1).

There is a good agreement for the invariant functions $F^{\pi^\pm}(x_F)$ in the range $x_F \geq 0.15$ for π^-p and $\nu(\bar{\nu})$p interactions [18]. In quark-parton models [21,22] the $F^{\pi^\pm}(x_F)$ distributions can be approxima-

---

* The charge-conjugate relations for quark fragmentations $D^{\pi^+}_{\bar{u}}(x_F) = D^{\pi^-}_{u}(x_F)$, $D^{\pi^-}_{\bar{u}}(x_F) = D^{\pi^+}_{u}(x_F)$ are taken into account.

** For K^N mesons the value $|x_F| \geq 0.1$ correspond to $x_E \geq 0.15$, but for Λ hyperons $x_E \geq 0.3$ at 40 GeV/c for average values of $\langle P_\perp \rangle$.

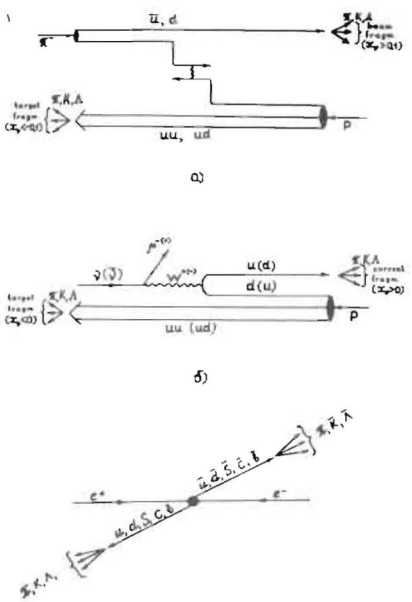

Fig.6. Scheme of π^-p (a), $\nu(\bar{\nu})$p (b) and e^+e^- interactions (c).

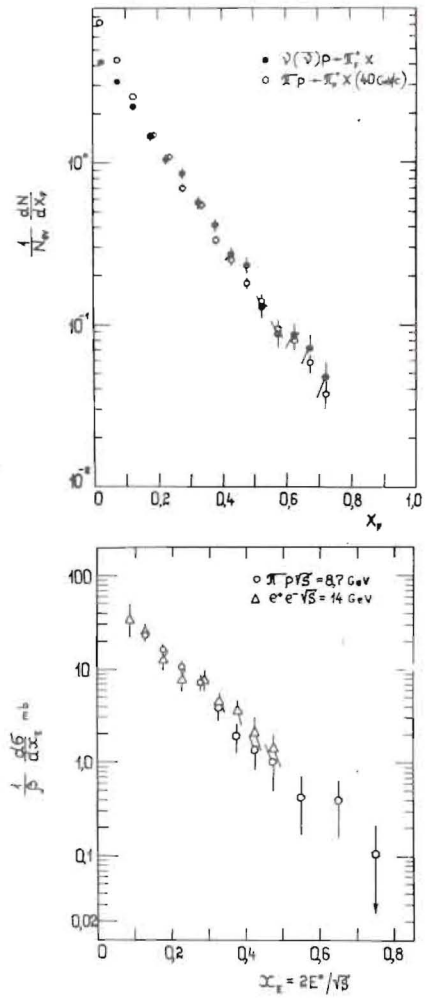

Fig.7. Fragmentation functions: • – $\frac{1}{2} D^{\pi^-}_{\nu p} + \frac{1}{2} D^{\pi^+}_{\bar{\nu} p}$, o – $D^{\pi^+}_{\pi^- p}$ for $x_F > 0$.

Fig.8. The $\frac{1}{\beta}\frac{d\sigma}{dx_E}$ distribution for K^N mesons produced in the forward hemisphere; • – for π^-p interactions ($\sqrt{S}$ = 8.7 GeV), Δ – for e^+e^- annihilation ($\sqrt{S}$ = 14 GeV).

ted by the function

$$F^{\pi^\pm}(x_F) = A\,(1 - |x_F|)^n , \qquad (8)$$

where A and n are free parameters (table 2). It is seen from table 2 that the values of n_{exp} are approximately equal for π^-p

Table 1. Approximation of the $D^{\pi^\pm}(x_F)$ function by the expression $A \exp(-B|x_F|)$.

Type of process	x_F range	A	B	χ^2/N
$\pi^-(x_F<0)$ ν,ν̄p	$-0.425 \le x_F \le -0.125$	5.5±0.6	9.4±0.5	4.9/7
π^-p	$-0.425 \le x_F \le -0.125$	5.1±0.2	9.0±0.2	4.8/7
$\pi^+(x_F>0)$ ν,ν̄p	$0.125 \le x_F \le 0.725$	4.6±0.3	6.5±0.2	9.1/10
π^-p	$0.125 \le x_F \le 0.725$	4.7±0.2	6.8±0.1	12.9/10
ν,ν̄p	$0.225 \le x_F \le 0.775$	5.5±0.4	4.9±0.2	13.3/12
$\pi^-(x_F>0)$ π^-p	$0.225 \le x_F \le 0.775$	4.2±0.2	4.4±0.1	62.6/12

Table 2. Approximation of the $F^{\pi^\pm}(x_F)$ function by the expression $A(1-|x_F|)^n$.

Type of process	x_F range	A	n_{exp}	χ^2/N	n_τ
$\pi^-(x_F<0)$ ν,ν̄p	$-0.525 \le x_F \le -0.225$	0.20±0.04	4.6±0.5	6.3/7	4÷5
π^-p	$-0.525 \le x_F \le -0.225$	0.17±0.01	3.6±0.2	1.3/7	
$\pi^+(x_F>0)$ ν,ν̄p	$0.225 \le x_F \le 0.775$	0.20±0.01	2.6±0.1	14.2/10	2
π^-p	$0.225 \le x_F \le 0.775$	0.17±0.07	2.3±0.1	20.7/10	
$\pi^-(x_F>0)$ ν,ν̄p	$0.325 \le x_F \le 0.775$	0.22±0.02	1.4±0.1	16.7/10	1
π^-p	$0.325 \le x_F \le 0.775$	0.138±0.006	0.83±0.06	26.3/10	

and $\nu(\bar{\nu})$p interactions, and they do not contradict the theoretically expected values of n_T [21,22].

b) Quark fragmentation into strange K^N and Λ particles

753 K°-mesons ($K^\circ_S \to \pi^+\pi^-$) and 345 Λ-hyperons ($\Lambda \to p\pi^-$) have been used for the analysis [23,24]. Figure 8 presents the $\frac{1}{\beta}\frac{d\sigma}{dx_E}$ function versus x_E for neutral K^N mesons produced in π^-p interactions in the forward hemisphere. A similar distribution of K^N mesons for e^+e^- interactions at $\sqrt{S}$ = 14 GeV [25] (the distributions are normalized to one another in the range $0.15 \leq x_E \leq 0.5$) is given there. The $\frac{1}{\beta}\frac{d\sigma}{dx_E}$ distributions of neutral K^N mesons produced in the quark fragmentation region in π^-p interactions are seen to have the same character as in e^+e^- collisions.

For $x_E \geq 0.15$ the $\frac{1}{\beta}\frac{d\sigma}{dx_E}$ distribution can be approximated by the dependence:

$$\frac{1}{\beta}\frac{d\sigma}{dx_E} = A \exp(-B|x_E|) . \qquad (9)$$

This yields B = 10+1 (table 3) which is approximately equal to that for e^+e^- annihilation (B = 8) [26].

For the quark-parton models of hadron-hadron collisions it is of interest to define $\lambda_S = \langle n_K \rangle / \langle n_\pi \rangle$, which determined the relation of strange and nonstrange quark pickup probability from the sea. This value is λ_S = 0.18+0.02 for x_E = 0.2÷0.5 which is in agreement with the data for e^+e^- annihilation ($\lambda_S \approx$ ≈0.17) [18,26,27].

Table 3

Values of parameter B

Particles	Forward	x^2/N	Backward	x^2/N
K^N-mesons, π^-p,40 GeV/c	10±1	0.5	9±1	0.73
Λ-hyperons, π^-p,40 GeV/c	8±3	0.6	3.6±0.4	0.4
Λ-hyperons, π^-p,16 GeV/c	10±1	0.8	4.4±0.3	0.87
K^N-mesons and Λ-hyperons e^+e^-	~8			

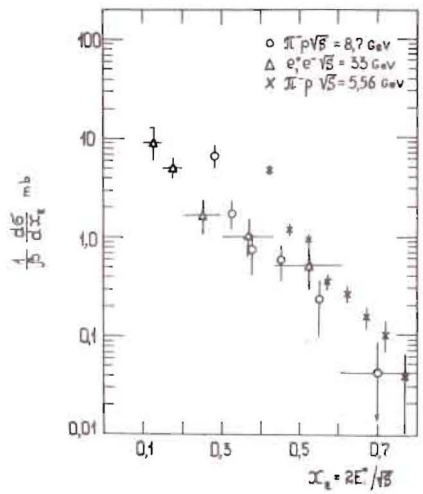

Fig.9. The $\frac{1}{\beta}\frac{d\sigma}{dx_E}$ distributions for Λ hyperons, produced in the forward hemisphere; o, × – π^-p interactions at $\sqrt{S}$ = 8.7 and 5.56 GeV; Λ – for e^+e^- annihilation ($\sqrt{S}$ = 33 GeV).

Fig.9 presents the $\frac{1}{\beta}\frac{d\sigma}{dx_E}$ distributions of Λ-hyperons for π^-p interactions in the forward hemisphere at 40 GeV/c and 16 GeV/c and for e^+e^- collisions at $\sqrt{s}$ = 33 GeV (the distributions are normalized over the range $0.3 \leq x_E \leq 0.6$) [27,28].

Table 3 shows the results of approximation of these distributions by eq.(9) in the range $x_E \geq 0.3$ (π^-p, 40 GeV/c), $x_E \geq 0.45$ (π^-p, 1.6 GeV/c) and $x_E \geq 0.1$ (e^+e^-, 33 GeV/c)* .

As is seen, the slopes of the $\frac{1}{\beta}\frac{d\sigma}{dx_E}$ distributions for the quark fragmentation into Λ particles over the range $x_F \geq 0.1$ for hadron-hadron and e^+e^- collisions are the same. For $x_E \geq 0.3 \div 0.45$ ($x_F \leq 0.1$) the deviation of the distributions from the obtained exponential dependence (10) for π^-p events (P = 40 GeV/c and 16 GeV/c) is likely to be due to the influence of the quark-quark interactions in the central region.

For the quark-parton models it is of interest to determine the ratio $\lambda_{qq} = \langle n_\Lambda \rangle / \langle n_K \rangle$ for quark fragmentation processes. A relative pickup probability of diquarks from the sea is characterized by this ratio. The multiplicity of K^N mesons over the range $0.3 \leq x_E \leq 0.6$ (in the forward hemisphere) for π^-p interactions at P = 40 GeV/c is equal to $\langle n_{K^N} \rangle$ = 0.026+0.04. Assuming that $\langle n_K \rangle = \langle n_{K^N} \rangle$, we obtain λ_{qq} = 0.14±0.03 for the quark fragmentation.

c) Diquark fragmentation for π^+ mesons

To analyse the diquark fragmentation in π^-p interactions, the $D^\pi(x_F)$ distributions of π^- mesons for the $x_F < 0$ region are compared with similar $\nu(\bar{\nu})$p data (6) (fig.10) [19]. As is seen, there is a good agreement, for the exception of the region $|x_F| \leq 0.15$, where the contribution from quark-quark interactions for π^-p

* For π^-p interactions at P = 16 GeV/c $x_E \geq 0.45$ corresponds to $|x_F| \geq 0.1$.

is singificant. The approximation of the $D^{\pi^-}(x_F<0)$ function by the dependence (7) yields the values of the parameters A and B which, coincide within errors, for both processes (table 1).

The result of approximation of the $F^{\pi^-}(x_F<0)$ distribution by the dependence (8) is given in table 2 [18]. The values of n_{exp} are approximately equal for π^-p and $\nu(\bar{\nu})p$ interactions and do not contradict the expected values.

It is also interesting to note that the $D^{\pi^\pm}(x_F)$ and $F^{\pi^\pm}(x_F)$ functions are broader in the region of quark fragmentation (the slopes are smaller) than in the region of diquark one.

From the data presented one can conclude that the difference of x_F spectra in the backward hemisphere in the c.m.s. for π^-p interactions and e^+e^- annihilation is due to the difference in the (x_F)distributions of secondary particles produced in quark and diquark fragmentation.

d) Diquark fragmentation into K^N mesons and Λ hyperons

Figures 11 and 12 present the $\frac{1}{\beta}\frac{d\sigma}{dx_E}$ distributions of K^N mesons and Λ hyperons produced in π^-p interactions in the backward hemisphere at P = 40 and 16 GeV/c [28].

The figures also show similar distributions for e^+e^- interactions at $\sqrt{s}$ = 14 and 33 GeV [27]. In addition, the $\frac{1}{\beta}\frac{d\sigma}{dx_E}$ distributions of K^N mesons and Λ hyperons in pp-interactions at P = 205 and 405 GeV/c [29,30] are also shown for one hemisphere in the region $x_E \geq 0.1$.

From the data presented the following conclusions can be drawn:

1. Within the experimental errors, the scaling behaviour of the $\frac{1}{\beta}\frac{d\sigma}{dx_E}$ function is observed for K^N mesons and Λ-hyperons produced in the diquark fragmentation region for π^-p and pp interaction from 16 to 405 GeV.

2. The $\frac{1}{\beta}\frac{d\sigma}{dx_E}$ distributions of K^N mesons, produced in the diquark fragmentation in hadron-hadron interactions for $0.15 \leq x_E \leq 0.5$, within the errors (~30%), are of the same character as the distributions of K^N mesons in e^+e^- collisions.

Approximating the $\frac{1}{\beta}\frac{d\sigma}{dx_E}$ distributions by the dependence (9) at $x_E \geq 0.15$ for K^N-mesons and at $x_E \geq 0.3$ for Λ-particles produced in π^-p collisions, we get $B_{K^N} = 9\pm1$ and $B_\Lambda = 3.6\pm0.4$ (table 3). For the distributions of K^N-mesons and Λ-hyperons in e^+e^- annihilation $B = 8$ [26].

It should be noted that the multiplicity of neutral K^N-mesons, produced in the diquark fragmentation region for π^-p in-

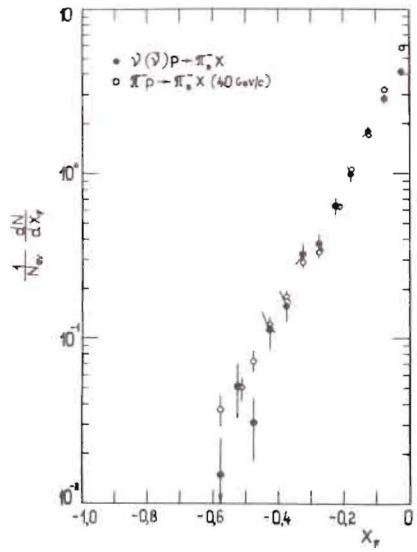

Fig.10. Fragmentation functions: ● – $\frac{1}{3}D^{\pi^-}_{\nu p} + \frac{2}{3}D^{\pi^-}_{\bar{\nu}p}$, o – $D^{\pi^-}_{\pi^- p}$ *for* $x_F < 0$.

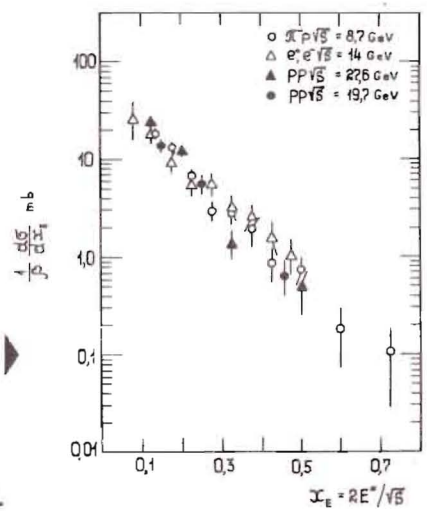

Fig.11. The $\frac{1}{\beta}\frac{d\sigma}{dx_E}$ *distributions for* K^N*-mesons produced in the backward hemisphere;* o – *for* π^-p *interactions* ($\sqrt{S}$ = *8.7 GeV);* Δ – *for* e^+e^- *annihilation* ($\sqrt{S}$ = = *14 GeV);* ▲, ● – *for* pp *interactions at* $\sqrt{S}$ = *27.6 and 19.7 GeV.*

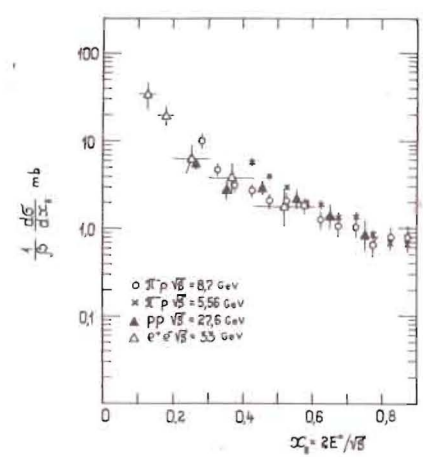

Fig.12. The $\frac{1}{\beta}\frac{d\sigma}{dx_E}$ *distributions for* Λ*-hyperons, produced in the backward hemisphere;* o, × – *for* π^-p *interactions at* $\sqrt{S}$ = *8.7 and 5.56 GeV;* ▲ – *for* pp *interactions* ($\sqrt{S}$ = *27.6 GeV);* Δ – *for* e^+e^- *annihilation* ($\sqrt{S}$ = *33 GeV).*

teractions ($\langle n_{K^0} \rangle = 0.039 \pm 0.03$ at $0.2 \leq x_E \leq 0.5$) is smaller than the multiplicity of their production in the quark fragmentation region. The multiplicity of Λ hyperons, produced in the diquark fragmentation region is approximately 4 times as large as that for the quark fragmentation (in the region $0.3 \leq x_E \leq 0.6$).

The value of $\lambda_S = \langle n_K \rangle / \langle n_\pi \rangle \sim 0.17$ for $\pi^- p$ interactions in the backward hemisphere at P = 40 GeV (for the diquark fragmentation) [18].

2.4. Average Charge of Hadron Jets

If, to a first approximation, one neglects the difference between $\bar{u}$ and d quarks interactions (fig.6a) and assumes that valency quarks (diquarks) fragmentize independently, then in the additive quark model [31] the average charge of jets, emitted forward in the c.m.s., is

$$\langle Q \rangle_F = \frac{1}{2} Q(\bar{u}) + \frac{1}{2} Q(d) + \langle Q_S \rangle = -0.5 . \qquad (10)$$

For particle jets, emitted backward in the c.m.s.,

$$\langle Q \rangle_B = \frac{1}{3} Q(uu) + \frac{2}{3} Q(ud) + \langle Q_S \rangle = \frac{5}{6} \approx 0.83 , \qquad (11)$$

where $\langle Q_S \rangle$ is the average charge of sea quarks which make a fragmenting quark and diquark colourless [32,33]. In this case a diquark is assumed to fragmentize into a baryon. To select hadron jets, which have quantum numbers of fragmenting quark (diquark) with large probability, it would be worthwhile to define Q depending on $x = \Sigma |x_{F_i}|$, where summation is performed over all charged particles in the jet, excluding the central region ($|x_{F_i}| \geq 0.1$).

Figure 13 presents the average charge of jets depending on x values for the forward and backward hemispheres. The charge has been defined in the following way: $\langle Q \rangle = \Sigma (N_+ - N_-)/N_{ev}$, where N_+ and N_- is the number of positive and negative particles in the jet, N_{ev} is the number of events with $n_\pm \geq 4$ multiplicity. In the same figure for comparison values are given for all charged secondly particles. As is seen from the figure, the charge of jets emitted forward at $x \geq 0.5$ does not contradict the expected value of $\langle Q \rangle = -0.5$. For jets emitted backward the value of $\langle Q \rangle$ approaches the expected one in the region $x \geq 0.8$ if hadrons with $|x_F| \leq 0.1$ are excluded.

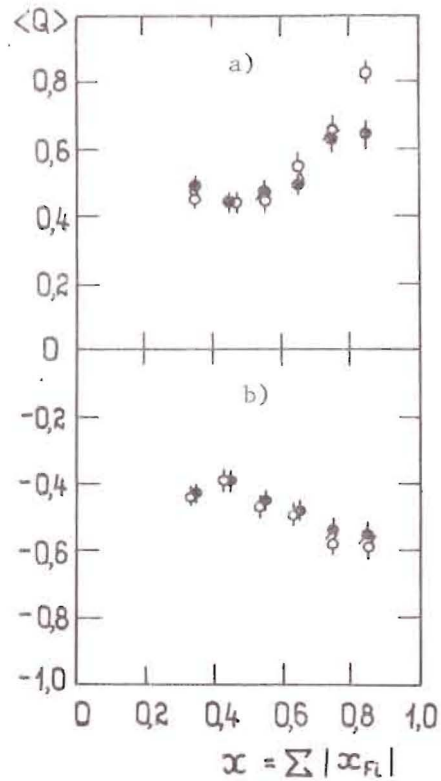

Fig.13. Dependence of average jet charge, $\langle Q \rangle$ on $x = \Sigma |x_{F_i}|$ in $n_\pm \geq 4$ events for $\pi^- p$ interactions; a) in the backward hemisphere; b) in the forward hemisphere. • – for all charged particles in events; o – for charged particles in events with $|x_F| \geq 0.1$.

Fig.14. Dependence of the average multiplicity of charged secondary particles: in the forward hemisphere n_F on particle multiplicity in the backward hemisphere n_B without diffraction processes (•) (a), the same for the dependence $n_B = f(n_F)$ (•) (b); ■ – for particles with $|x_F| \geq 0.1$; ▲ – for particles with $|x_F| < 0.1$. The full line is the fit of the data by the formula (12).

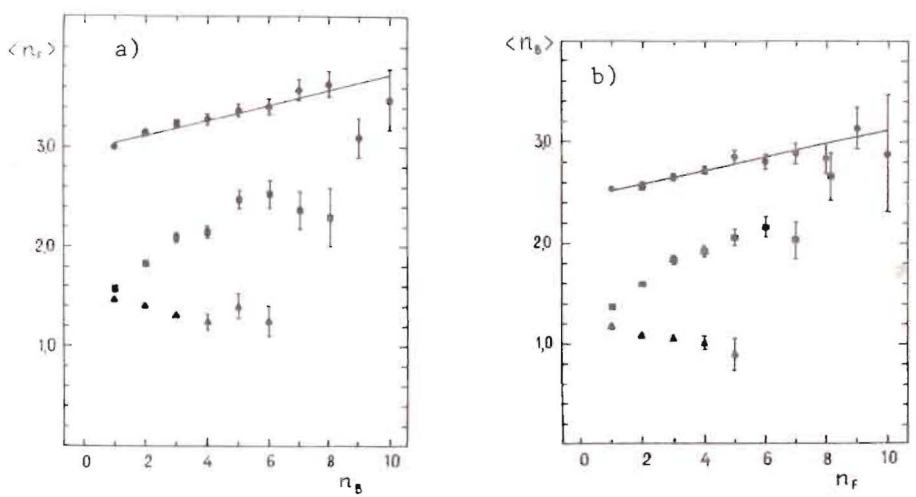

2.5. Multiplicity Correlations Between Particles Emitted to the Forward and Backward Hemispheres in the c.m.s.

The study of multiplicity correlations between particles, emitted forward and backward in the c.m.s. can give interesting information on long-range correlations in soft hadron-hadron collisions.

Figure 14 shows the average multiplicities of particles $\langle n_F \rangle (\langle n_B \rangle)$ in one hemisphere versus the multiplicities of particles $n_B(n_F)$ in the other hemisphere. As is seen, there are some correlations between multiplicities of particles emitted forward and backward in the c.m.s. Presented here are similar results separately for particles produced in both central ($|x_F| \leq 0.1$) and fragmentation ($|x_F| > 0.1$) regions. It is seen that the production of fast particles in the opposite hemispheres is not correlated with each other, but substantial correlations are observed for slow particles. Similar results have been obtained for K^-p and pp interactions [34,35].

Table 4 presents the results of approximation of obtained dependences by the linear function:

$$\langle n_{F(B)} \rangle = a + b n_{B(F)} , \qquad (12)$$

where a and b are free parameters.

Table 4

Experimental values of parameters a , b in the formula (12)

$a_F = 2.97 \pm 0.03$	$b_F = 0.07 \pm 0.01$	$x^2/N = 10.5/10$
$a_B = 2.46 \pm 0.03$	$b_B = 0.06 \pm 0.01$	$x^2/N = 4.5/10$

The correlations under study are described by the model based on schemes of dual topological unitarization [36,37] in which they are due to the overlap of particles from the decays of two clusters emitted in the opposite directions.

It is experimentally shown [38] that the obtained correlations are defined by slow ($|x_F| \leq 0.1$) particles of opposite charge which is connected with the well-known short-range correlations of these particles. The decays of slow (in the c.m.s.) resonances can be the source of this correlations. Fast particles ($|x_F| > 0.1$) are produced independently.

These data show that the fragmentation of quarks and diquarks in meson-nucleon interactions occurs independently.

Thus, the whole analysis given above indicates that the mechanism of quark and diquark hadronization in π^-p, $\nu(\bar{\nu})p$ interactions and e^+e^- annihilation is universal.

3. ANALYSIS OF THE HADRON JET BEHAVIOUR IN π^-C INTERACTIONS AT P = 40 GeV/c

Figure 15 presents a possible diagram of hadron jet fragmentative production in cumulative π^-C interactions. Unlike the diagram of π^-p interactions (fig.6a), the production of secondary particle jets in the backward hemisphere in the c.m.s. (fragmentation region of target nucleus) in cumulative π^-C interactions can be considered as a result of quark and diquark fragmentation from multiquark states of carbon nuclei.

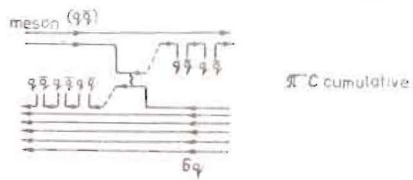

Fig.15. Scheme of cumulative interactions.

Multinucleon π^-C interactions with the total charge of secondary particles Q = +1,+2,+3,+4 were selected for analysis.

For each group of multinucleon interactions with charge Q the analysis was performed in the c.m.s. of incident π^--meson and the corresponding number of interacting nucleons $\langle \nu_n \rangle$ [39].

The energy of collision is defined by the formula

$$E_{c.m.s.} = \sqrt{S} = \sqrt{2\nu_n m_N E_\pi} , \qquad (13)$$

with m_N the nucleon mass and E the energy of incident pion.

The cumulative events were selected using the variable β_i [5]

$$\beta_i = \frac{E_i - P_{||_i}}{m_N} , \qquad (14)$$

where E_i and $P_{||_i}$ are the energy and longitudinal momentum of secondary particles in the lab.system. According to the established selection criteria [41], an event was assumed to be cumulative if a π^+ meson with $\beta_i \geq 0.6$ or a proton with $\beta_i \geq 1$ was registered in it. However, the hadronization of quarks from multiquark nuclear states can occur so that none of the particles has the value of β_i outside the kinematical limit of pion-nucleon collision whereas the sum of all β_i in a jet, produced in quark hadronization, is larger than 1:

$$\beta_0 = \sum_i \beta_i > 1.0 . \qquad (15)$$

Thus, cumulative processes were selected according to the condition (15). A group of particles, emitted backward in the c.m.s. of ($\pi^- \nu_n$)interactions and satisfying the condition (15), was assumed to be a cumulative jet. The number of cumulative events thus selected was 2419 and their fraction of all π^-C interactions ~18%.

3.1. Jet Production

The jet particle production in π^-C interactions has been studied using the variable S.

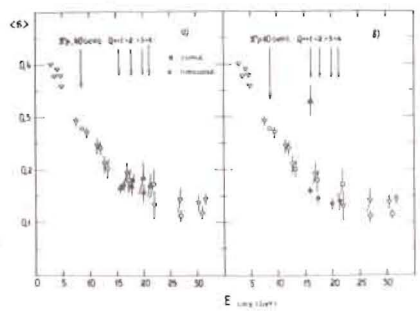

Fig.16. Dependence of average values of sphericity <S> for various types of interactions on energy in the c.m.s.; ▽, □ – for e^+e^- annihilation; for hadron jets emitted forward (a) and backward (b) in the c.m.s. for cumulative (●) and noncumulative (▲) π^-C interactions.

Figure 16 shows average values of <S> versus $E_{c.m.s.}$ for the secondary particle jets collimated towards a primary pion and in an opposite direction in cumulative ($\beta_0 > 1.0$) and noncumulative ($\beta_0 \leq 1.0$) events. The particles with $|x_F| = 2P^*_{||} / E_{c.m.s.} \geq 0,5$, are assigned to jets. As is seen from the figure, the value of <S> for both jets in cumulative interactions agrees with the e^+e^- data [12,13,15] at equal energies in the c.m.s. For noncumulative events one can see a disagreement with similar data on e^+e^- interactions for the hadron jets produced in the fragmentation region of target nucleus. Therefore one can say that there is another mechanism of their production. Figure 3 presents the average multiplicity dependence of charged particles in e^+e^- annihilation on energy in the c.m.s. [12]. Average values of $<n_\pm>$ for cumulative events with $\beta_0 > 1.0$ versus energy in the c.m.s. are shown in the same figure. It is seen that the $<n_\pm>$multiplicity in cumulative processes grows with increasing $\sqrt{S}$ and coincides within the experimental errors with the $<n_\pm>$ value for e^+e^- interactions at equal energies.

3.2. Characteristics of Charged Particles in Jets

Figure 17 shows the transverse momentum squared distributions of charged particles relative to the jet axis in cumulative π^-C interactions with Q = +1 and in e^+e^-annihilation. These $dN/dP_\perp^2$

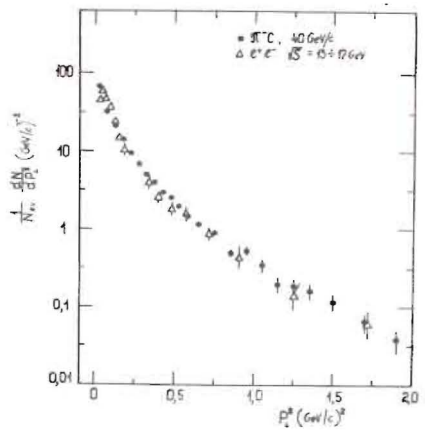

Fig.17. Transfer squared momentum distribution of charged particles relative to the jet axis, ● – for cumulative π^-C interactions (Q = +1), Δ – for e^+e^- annihilation at $\sqrt{S}$ = 13÷17 GeV.

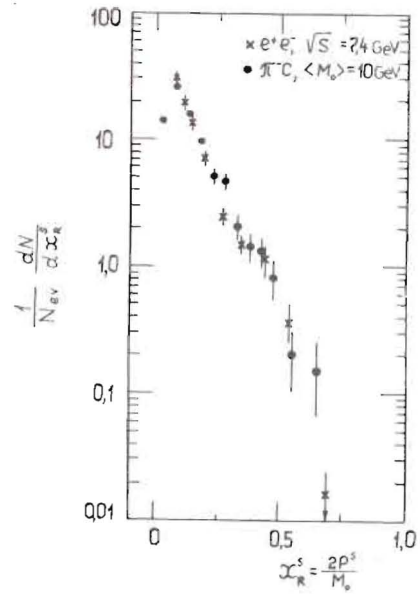

Fig.18. The x_R^S distribution of pions in cumulative π^-C collisions with charge Q = +1 in the own rest frame with $<M_0> \approx$ ≈ 10 GeV (backward hemisphere); x – the same distribution of pions in e^+e^- interactions $E_{c.m.s.}$ = 7.4 GeV.

distributions are similar for both types of the interactions considered.

Comparison of the x_F distributions of secondary particles in the forward and backward hemispheres in the c.m.s. of cumulative π^-C interactions with e^+e^-data shows that there is a good agreement in the forward hemisphere, whereas they differ in the backward [39].

This difference can be due to variations of initial states of interacting objects which lead to various compositions of secondary particles in the final state and to distinctions in their phase space distributions (analogous to the difference of quark and diquark fragmentation (§2)). Therefore it would be more correct to compare identical systems of secondary particles in the final state (in this case the meson subsystem) in their rest frame. With this aim the events with two identified protons were selected from cumulative π^-C interactions with Q = +1. The protons were excluded from the analysis. The energy of the remaining meson subsystem, $<M_0>$, equals to 10 GeV.

Figure 18 illustrates the $x_R^S = 2P^S/M_0$ distribution of charged pion, where P^S is the total momentum of pions in their rest frame. It is seen that this distribution coincides within the experimental errors with a similar distribution of pions in e^+e^- annihilation.

3.3. Quark and Diquark Fragmentation into Strange Particles

550 K_S^0 meson ($K_S^0 \to \pi^+\pi^-$) and 294 Λ hyperons ($\Lambda \to p\pi^-$) were used for analysis [41].

a) Fragmentation of quarks into strange particles

Figures 19 and 20 present the $\frac{1}{\beta}\frac{d\sigma}{dx_E}$ function versus x_E for K^N mesons and Λ-hyperons produced in cumulative processes in the forward hemisphere in the c.m.s. of $\pi^-\nu_n$ collisions. Similar distributions for neutral strange particles in π^-p and e^+e^- interactions are given in the same figures [26,27]. The distributions of K^N mesons and Λ hyperons in e^+e^- and π^-p interactions are normalized so that the square of the considered region x_E may be similar to the one in π^-C interactions. From the digures one can see that, the dependence of the function $\frac{1}{\beta}\frac{d\sigma}{dx_E}$ on x_E for K^N mesons and Λ hyperons in cumulative π^-C, π^-p and e^+e^- interactions is similar within the experimental errors. The approximation of these distributions by the dependence (9) for cumulative π^-C interactions yields $B_{K^N} = 9\pm2$ and $B_\Lambda = 13\pm4$ (table 3). From the table it is seen that they coincide within the experimental errors, with similar values for π^-p and e^+e^- interactions.

b) Diquark fragmentation into strange particles

To compare the properties of K^N mesons and Λ hyperons produced in the target-nucleus fragmentation region in cumulative processes with the π^-p and e^+e^- data, we have selected a subsystem consisting of mesons and one baryon [39]. Then the production of Λ hyperons and K^N-mesons in the backward hemisphere in the rest frame of the selected subsystem can be considered as a result of the fragmentation of uu, ud and dd diquarks from multiquark states of the carbon nucleus. The energy of the selected subsystem of secondary particles, $\langle M_0 \rangle$, was $\approx$12.3 GeV. Figures 21 and 22 show the $\frac{1}{\beta}\frac{d\sigma}{dx_E^S}$ function versus x_E^S for K^N mesons and Λ hyperons produced in the target nucleus fragmentation region for cumulative π^-C interactions with $Q = +1,+2$. Here $x_E^S = 2E^S/M_0$ and E^S is the energy of particles in the rest

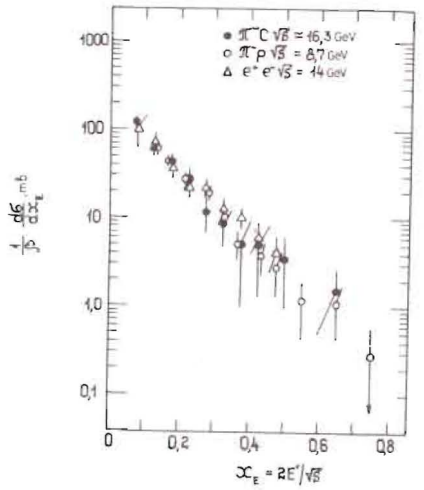

Fig.19. The $\frac{1}{\beta}\frac{d\sigma}{dx_E}$ distribution for K^N-mesons produced in the forward hemisphere in the c.m.s. of cumulative π^-C(●) ($\sqrt{s}$ = 16.3 GeV), π^-p(○) ($\sqrt{s}$ = 8.7 GeV) and e^+e^- interactions (△) ($\sqrt{s}$ = 14 GeV).

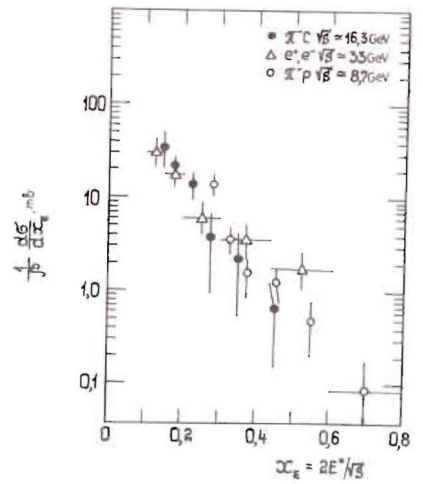

Fig.20. The $\frac{1}{\beta}\frac{d\sigma}{dx_E}$ distribution for Λ-hyperons, produced in the forward hemisphere in the c.m.s. of cumulative π^-C(●) ($\sqrt{s}$ = 16.3 GeV), π^-p(○) ($\sqrt{s}$ = 8.7 GeV) and e^+e^- interactions (△) ($\sqrt{s}$ = 33 GeV).

frame of subsystem M_0. As is seen from the figures, the presented $\frac{1}{\beta}\frac{d\sigma}{dx_E^S}$ distributions for strange particles in the x_E^S region for cumulative π^-C, π^-p, and e^+e^- interactions are in agreement within the experimental errors. The values of parameters B_K and B_Λ equal to 8+4 and 5.2+0.7 obtained by approximating these distributions by the dependence (9) agree, within the experimental errors, with the π^-p data. For Λ hyperons produced in the region of quark fragmentation in π^-p and cumulative π^-C interactions the value of parameter B is smaller than that for e^+e^- annihilation.

The analysis performed means that quark and diquark fragmentation into π mesons and strange particles in cumulative interactions on light nuclei and in soft hadron collisions is similar. Quark fragmentation into the same particles in these interactions is similar to the one in e^+e^- annihilation.

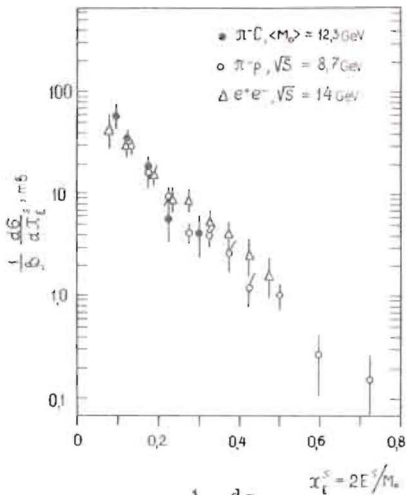

Fig.21. The $\frac{1}{\beta}\frac{d\sigma}{dx_E^S}$ *distribution for* K^N *mesons, produced in the backward hemisphere in the rest frame of the subsystem* (M_0)*: in cumulative* π^-C *interactions* (•) ($\langle M_0 \rangle$ = *= 12.3 GeV); in the c.m.s. of* π^-p (○) ($\sqrt{S}$ *= 8.7 GeV) and* e^+e^-(Λ) ($\sqrt{S}$ *= 14 GeV) interactions.*

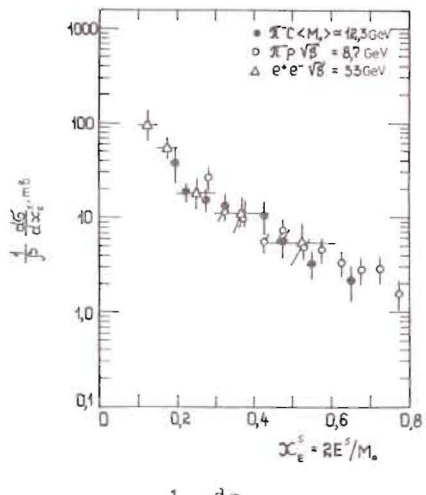

Fig.22. The $\frac{1}{\beta}\frac{d\sigma}{dx_E^S}$ *distributions for* Λ*-hyperons in the backward hemisphere in the rest frame of the separated subsystem* (M_0) *in cumulative* π^-C *interactions* (•) ($\langle M_0 \rangle$ = *= 12.3 GeV); in the c.m.s. of* π^-p (○) ($\sqrt{S}$ *= 8.7 GeV) and* e^+e^-(Λ) ($\sqrt{S}$ *= 33 GeV) interactions.*

4. DESCRIPTION OF HADRON JET PROPERTIES IN RELATIVE 4-VELOCITY SPACE

Traditional analysis of the jet behaviour of secondary particles using variables "sphericity", "thrust" and other is usually performed in the c.m.s. of interacting particles. These variables are not Lorentz invariant, their values depend strongly on the frame system, which is connected with the physics of a process. In each individual case it is difficult to define the c.m.s. in hadron-nucleus and nucleus-nucleus interactions.

Thus, to analyse the behaviour of particle jets, it is necessary to use a relativistic-invariant definition of hadron jets. As a relativistic invariant variable, one can use the square of relative 4-velocities of two particles (i-th and k-th)[42]

$$b_{ik} = -\left(\frac{P_i}{m_i} - \frac{P_k}{m_k}\right)^2 . \qquad (16)$$

Here P_i, P_k are 4-momenta of i-th and k-th particles and m_i, m_k are their masses of inclusive processes

$$I + II \to 1 + 2 + \ldots \qquad (17)$$

Indices i and k may refer both to colliding objects (I,II) and to secondary particles 1,2 and so on.

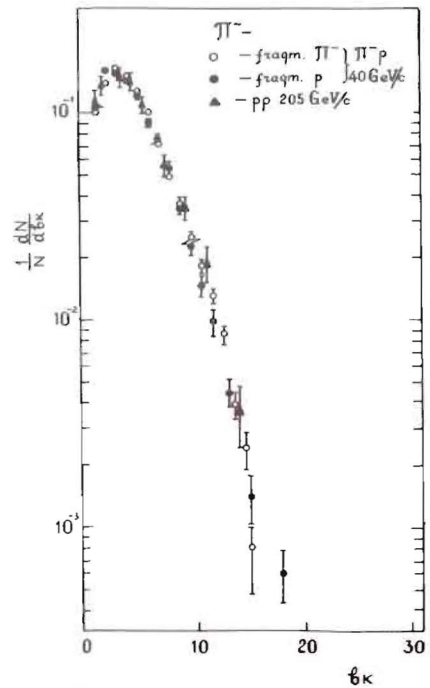

Fig.23. The b_k *distribution of* π^- *mesons relative to the jet axis produced in the fragmentation region of an incident pion (○) and of a proton* p (•) *in the* π^-p *interactions.* (▲) *the same distribution for* pp *collisions at* P = 205 *GeV/c.*

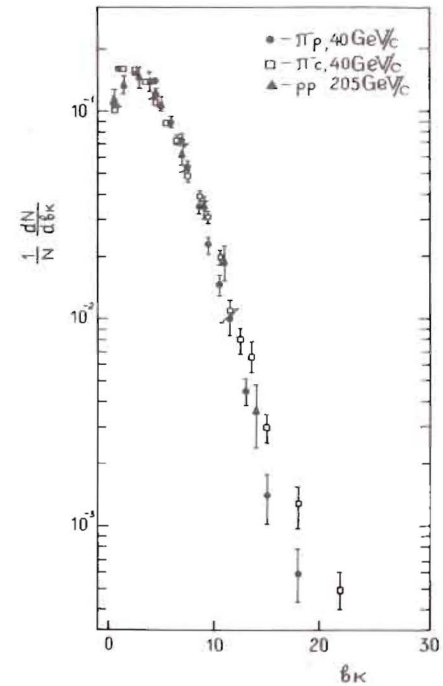

Fig.24. The b_k *distribution of* π^- *mesons relative to the jet axis produced in the target fragmentation region in* (•) $-\pi^-p$, (□) $-\pi^-C$ *interactions at of 40 GeV/c and* (▲) – pp *collisions at* P = 205 *GeV/c.*

A jet is considered as a cluster of hadrons with relatively small values of b_{ik}.

A unit four-dimensional vector is used as a jet axis[43].

$$V = \frac{\sum_i u_i}{\sqrt{(\sum_i u_i)^2}}, \quad \text{where} \quad u_i = \frac{P_i}{m_i} \qquad (18)$$

Summation is performed over all particles from the selected group of particles. It is proposed to analyse the distribution of particles in jets by the variable:

$$b_k = -(V - u_k)^2 \ . \qquad (19)$$

Figure 23 shows the distribution of π^- mesons in π^-p interactions for jets produced in the fragmentation regions of an incident π^- meson and of a proton. The particles with $|x_F| \geq 0.1$ are assigned to a jet. One can see from the figure, that both obtained distributions coincide, within the errors, i.e., quark and diquark fragmentation into pions is similar in the relative four velocity.

Figure 24 shows the b_k distributions of π^- mesons in the jets produced in the region of target fragmentation for π^-p, π^-C interactions at 40 GeV/c and for pp -interactions at P = = 205 GeV/c (the data have been obtained using a hydrogen bubble chamber at the Argonne Laboratory).

Table 5

Average values of the variable b_k for π^- mesons

Region of jet production	π^-p	π^-C	pp
Bean fragmentation	4.21±0.03	4.19±0.04	4.5±0.1
Target fragmentation	4.06±0.04	4.36±0.04	4.5±0.1

One can see that the b_k distributions of π^- mesons in the considered jets are the same within the experimental errors. Average values of the variable b_k for different types of interactions are given in table 5. It is seen that these values are small $\langle b_k \rangle < 5$ and they depend within 10% neither on the type of interaction nor on the primary energy of collision over the energy range under study.

Thus, it looks more promising in the future to use relativistic invariant b_{ik} variables for studies of properties of hadron jets produced in nuclear interactions.

The authors are grateful to the staff of the 2m Propane Bubble Chamber Collaboration for their help in the work and useful discussions.

REFERENCES

1. Basile M. et al. Nuovo Cim., 1980, 58A, p.193; 1981, 65A, p.414; 1981, 65A, p.400; 1982, 67A, p.244; 1982, 67A, p.53.
2. Gottgens R. et al. Nucl.Phys., 1981, B178, p.392.
3. Barth M. et al. Nucl.Phys., 1981, B192, p.289.
4. Baldin A.M. ECHAYA, 1977, 8, p.429.
5. Stavinsky V.S. ECHAYA, 1979, 10, p.949; JINR, P2-80-767, Dubna, 1980.
6. Gavrilov V.G., Leksin G.A. Elementary Particles. X School of ITEF. Energoizdat, M., 1983, p.46.
7. Abdurakhimov A.U. et al. JINR, P1-6326, Dubna, 1972; Yad.Fiz., 1973, 18, p.545; Nucl.Phys., 1974, B79, p.57.
8. BBCDSSTTU-BW Collaboration. Phys.Lett., 1972, 39B, p.371.
9. Angelov N. et al. Yad.Fiz., 1977, 25, p.1013.
10. Brandt S., Dahmen H.D. Z.Phys., 1979, C1, p.61.
11. Schwitters R.F. et al. Phys.Rev.Lett., 1975, 35, p.1320; Hanson G.G. et al. Phys.Rev.Lett., 1975, 35, p.1609.
12. Berger Ch. et al. Phys.Lett., 1979, 81B, p.410; Phys.Lett., 1978, 78B, p.176; Phys.Lett., 1979, 82B, p.449.
13. Brandelik R. et al. Phys.Lett., 1979, 83B, p.261.
14. Grishin V.G. et al. Yad.Fiz., 1983, 37(4), p.915; JINR, P1-81-542, Dubna, 1981; JINR, P1-82-252, Dubna, 1982.
15. Wolf G. DESY 80/85, Sept.1980; Int.Conf. on High Energy Phys., Geneva, 1979, vol.1, p.220.
16. Hanson G. SLAC-PUB-1814, September, 1976.
17. Grishin V.G. et al. JINR, P1-83-306, Dubna, 1983.
18. Grishin V.G. et al. JINR, P1-83-823, Dubna, 1983; JINR, E1-84-263, Dubna, 1984; JINR, P1-84-79, Dubna, 1984; Yad.Fiz., 1984, 40, 4(10), p.936; Yad.Fiz., 1985, 41, 3, p.684.
19. Allen P. et al. Nucl.Phys., 1983, vol.B214, No.3, p.369.
20. Drell S.D. et al. Phys.Rev., 1969, 187, p.2159; Phys. Rev., 1970, D1, p.1617.
21. Gunion J.F. Proc. 11 Int. Symp. on Multipart. Dynamics, Bruges, 1980, p.767.
22. Anderson B., Gustafson G., Reterson C. Phys.Lett., 1977, 69B, p.221; 1977, 71B, p.337.
23. Abdurakhimov A.U. et al. JINR, 1-6967, Dubna, 1973; JINR, P1-7267, Dubna, 1973; Yad.Fiz., 1973, 18, p.1251.
24. Angelov N. et al. JINR, P1-81-5, Dubna, 1981.
25. Breakstone A. et al. CERN/EP 81-68, Rev.July, Geneva, 1981.
26. Wolf G. DESY 81-086, Dec., 1981.
27. Oberlak H. MPI-PAE/EXP E1110, Sept., 1982.
28. Balea E. et al. JINR, 1-81-38, Dubna, 1974; Balea E. et al. Nucl.Phys., 1980, B163, p.21.
29. Jaeger K. et al. Phys.Rev., 1975, D11, p.2405.

30. Kachimi H. Phys.Rev., 1979, D20, p.37.
31. Anisovich V.V., Shekhter V.M. Nucl.Phys., 1973, B55, p.455.
32. Feynman R.P. Photon-Hadron Interactions. "Mir", M., 1975.
33. Kartvelishvili V.G., Roinishvili V.N. Preprint HEPI, 81-14, Serpukhov, 1981.
34. Gottgens R. et al. Z.Phys.C, 1981, 11, p.189.
35. Kafka T. et al. Phys.Rev.Lett., 1975, 34, p.687.
36. Dias de Deus J., Jadack S. Acta Phys.Pol., 1978, B9, p.249.
37. Capella A. et al. Phys.Lett., 1979, 81B, p.68.
38. Grishin V.G. et al. JINR, P1-85-259, Dubna, 1985.
39. Grishin V.G. et al. JINR, P1-82-393, Dubna, 1982; Yad. Fiz., 1983, vol.38, 3(9), p.687; Baldin A.M. et al. JINR, P1-83-483, Dubna, 1983; Yad.Fiz., 1984, vol.39, 5, p.1215; Grishin V.G. et al. JINR, P1-84-205, Dubna, 1984; Yad.Fiz., 1985, vol.41, 2, p.371; Baldin A.M. et al. JINR, E1-84-317, Dubna, 1984.
40. Anoshin A.I. et al. Yad.Fiz., 1982, vol.36, p.409.
41. Angelov N. et al. Yad.Fiz., 1977, vol.25, p.350; Yad.Fiz., 1976, vol.24, p.732.
42. Baldin A.M. DAN SSSR, 1975, vol.222, p.1064; Nucl.Phys., 1985, A434, p.695c.
43. Baldin A.M., Didenko L.A. In: JINR Rapid.Comm., No.3, Dubna, 1984, p.5.

Received by Publishing Department
on May 31, 1985.

Балдин А.М. и др. E1-85-415
Универсальность струй адронов в мягких и жестких взаимодействиях частиц при высоких энергиях

Изучается образование струй адронов в мягких $\pi^- p$-и кумулятивных $\pi^- C$-взаимодействиях при импульсе 40 ГэВ/с. Анализируются коллективные характеристики струй, а также функции фрагментации кварков и дикварков в заряженные пионы и нейтральные странные частицы. Полученные результаты сравниваются с аналогичными данными для e^+e^--и $\nu(\bar{\nu})p$-столкновений. Свойства адронных струй изучаются также с помощью релятивистски-инвариантных переменных - квадратов четырехмерных относительных скоростей $b_{ik} = -(\frac{P_i}{m_i} - \frac{P_k}{m_k})^2$. Полученные результаты указывают на то, что фрагментация кварков /дикварков/ в мягких адрон-адронных столкновениях, кумулятивных взаимодействиях на легких ядрах, в e^+e^--аннигиляции и в глубоконеупругом $\nu(\bar{\nu})p$-рассеянии происходит одинаковым образом.

Работа выполнена в Лаборатории высоких энергий ОИЯИ.

Препринт Объединенного института ядерных исследований. Дубна 1985

Baldin A.M. et al. E1-85-415
Universality of Hadron Jets in Soft and Hard Particle Interactions at High Energies

The hadron jet production in soft $\pi^- p$-and cumulative $\pi^- C$-interactions at a 40 GeV/c momentum is studied. The collective characteristics of jets and the functions of the quark and diquark fragmentation into charged pions and neutral strange particles are analysed. The results obtained are compared with analogous data for e^+e^--and $\nu(\bar{\nu})p$-interactions. The hadron jet properties are also studied using relativistic invariant variables - the squared relative 4-velocities $b_{ik} = -(\frac{P_i}{m_i} - \frac{P_k}{m_k})^2$. The results obtained show that the quark (diquark) fragmentation proceed in a similar manner in soft hadron-hadron collisions, cumulative interactions on light nuclei, in e^+e^--annihilation and deep inelastic $\nu(\bar{\nu})p$-scattering.

The investigation has been performed at the Laboratory of High Energies, JINR.

Preprint of the Joint Institute for Nuclear Research. Dubna 1985